NASA TECHNICAL NOTE

NASA TN D-5127

A TECHNIQUE FOR IDENTIFYING PILOT DESCRIBING FUNCTIONS FROM ROUTINE FLIGHT-TEST RECORDS

by Rodney C. Wingrove and Frederick G. Edwards

Ames Research Center
Moffett Field, Calif.

NATIONAL AERONAUTICS AND SPACE ADMINISTRATION • WASHINGTON, D. C. • MAY 1969

NASA TN D-5127

A TECHNIQUE FOR IDENTIFYING PILOT DESCRIBING FUNCTIONS FROM ROUTINE FLIGHT-TEST RECORDS

By Rodney C. Wingrove and Frederick G. Edwards

Ames Research Center
Moffett Field, Calif.

NATIONAL AERONAUTICS AND SPACE ADMINISTRATION

For sale by the Clearinghouse for Federal Scientific and Technical Information
Springfield, Virginia 22151 – CFSTI price $3.00

TABLE OF CONTENTS

A TECHNIQUE FOR IDENTIFYING PILOT DESCRIBING FUNCTIONS FROM ROUTINE FLIGHT-TEST RECORDS

By Rodney C. Wingrove and Frederick G. Edwards

Ames Research Center

SUMMARY

Previous studies have shown that the dynamic response of the pilot can be represented by a linear element (describing function) and a remnant term (output noise). The previous work also has indicated that there is an error in identifying the pilot describing function from routine tracking task records because the output noise of the pilot transfers through the control loop, producing an undesired correlation with his input signal. This report shows that this correlation, and thus the identification error, can be reduced by shifting the input signal during the computer processing an amount equivalent to the effective time delay of the pilot. This report includes a theoretical analysis of this technique and examples to illustrate its application.

The theoretical analysis considers the fact that the computer processing is constrained to identify only physically realizable systems. With this constraint, it is shown that the error in identifying the pilot describing function depends on the spectrum of the pilot's output noise; the identification error can be made small if the noise is near "white" in relation to the sum of all effective time delays through the control loop (pilot plus controlled element). This result is significant because, if these conditions are met, it is possible to identify the describing function of the pilot in a feedback system that is excited only by his output noise.

The identification of several simulated pilot models is included in this study to illustrate this technique. Also, representative data from the retrofire phase of the Gemini X flight have been analyzed and are presented to demonstrate the successful application of this technique with routine spacecraft operating records.

INTRODUCTION

This report considers the problem of identifying the input-output relationship of the pilot by use of measured data from routine flight operations in which the pilot provides feedback control. The problem in using the measured input and output data directly is that any extraneous output noise by the pilot causes an error in identification. This problem is solved in this report by the development of a computer processing technique that, under certain conditions, yields an estimate relatively free from identification error.

Since the identification of feedback control systems is important in many fields, the technique has wide significance and applicability.

The input-output characteristic of a pilot must be regarded as random, nonlinear, and dependent on the task he is to perform. Many previous studies have shown that this type of response can be represented appropriately with a quasi-linear system modeled by a linear element (describing function) and a remnant term (output noise). The pilot describing functions usually have been identified from records obtained in ground-based simulators (ref. 1) and flight tests (ref. 2) wherein carefully controlled external forcing functions are used to excite the pilot-vehicle system. The pilot describing functions are measured by comparing the input and output signals of the pilot with the known forcing function. This method minimizes those errors in identification due to any correlation of the input signal with the pilot's output noise. Reference 3 contains a good review of this previous work and summarizes the measured pilot describing functions.

Most other methods for measuring pilot describing functions depend on random disturbances (e.g., aerodynamic turbulence, propulsive disturbance, etc.) to excite the pilot-vehicle system. These methods compute directly the describing function of the pilot from his input and output signals. However, there is a fundamental difficulty with these methods because the pilot's output noise transmitted through the control loop produces an undesired correlation between his input and output signals, thereby causing an error in identification. In reference 4, the expected error is analyzed and it was shown that if the amplitude of the pilot's noise is large, as compared with the external disturbance, then the identification error is unacceptable.

During routine flight-test operations, there are no carefully controlled forcing functions and even the random external disturbance may be quite small so that the principal system excitation may come from the pilot's output noise. This report shows that in such situations it may still be possible, under certain reasonable conditions, to determine the pilot describing function without incurring an unacceptable identification error. One required condition is that the pilot (or possibly the feedback control loop) have a time delay. If this condition is met, it is possible to take advantage of this fact in the identification data processing. In effect, the input signal is shifted during processing by an amount equal to the time delay of the pilot. Although previous studies (refs. 5-7) have considered the use of a time shift in the measurement of pilot describing functions, it was apparently not observed that this time shift would strongly influence the error in identification.

This report presents a theoretical analysis to show that this technique will reduce the identification error. The simulation and identification of several known system elements are included to compare with the theory and to illustrate the use of this technique. Also, results obtained from the retrofire phase of the Gemini X mission are presented to demonstrate the application of this technique to routine flight-test records.

NOTATION

$c(t)$	controller deflection (output of pilot)
$e(t)$	error signal (input to pilot)
$F[\ ]$	Fourier transform of [ ]
$i(t)$	external disturbance
K	constant gain
$N_c(j\omega)$	numerator terms in $Y_c(j\omega)$
$n(t)$	internal noise (pilot remnant)
$R_{ec}(\tau)$	cross-correlation function of $e(t)$ and $c(t)$
$R_{en}(\tau)$	cross-correlation function of $e(t)$ and $n(t)$
$R_{ee}(\tau)$	autocorrelation function of $e(t)$
$R_{nn}(\tau)$	autocorrelation function of $n(t)$
t	time, sec
$Y_c(j\omega)$	controlled element describing function
$Y_m(j\omega)$	measured describing function (ideal)
$\hat{Y}_m(j\omega)$	measured describing function (actual)
$Y_p(j\omega)$	pilot describing function
$\hat{Y}_p(j\omega)$	estimated pilot describing function
α	exponential decay factor, sec^{-1}
$\varepsilon(t)$	residual
λ	time shift used during analysis, sec
τ_c	time delay in $Y_c(j\omega)$, sec
τ_p	time delay in $Y_p(j\omega)$, sec
$\Phi_{ee}(\omega)$	power spectrum of $e(t)$
$\Phi_{nn}(\omega)$	power spectrum of $n(t)$
$\Phi_{ec}(j\omega)$	cross-power spectrum of $e(t)$ and $c(t)$

$\Phi_{en}(j\omega)$ cross-power spectrum of e(t) and n(t)

ω frequency, rad/sec

BACKGROUND

This section discusses the piloted control system elements and indicates the error in identifying the pilot describing function from routine tracking task records. A computing process for reducing this identification error is then outlined. This background material precedes a more detailed analysis of the identification error presented later in the report.

General Remarks

Figure 1 is a block diagram of the pilot in a compensatory tracking task trying to control his output c(t) so that the input error signal e(t)

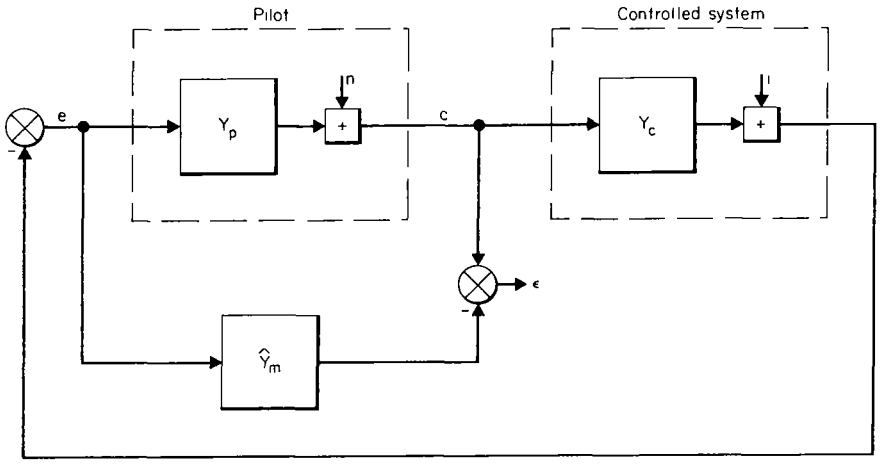

Figure 1.- Identification using standard measurement methods.

is kept near zero. Generally, the input-output characteristics of the pilot must be considered as complex, nonlinear, and time varying. However, for the purposes of modeling, it is common practice to assume that his characteristics can be represented by a quasi-linear system (ref. 3). This mathematical model contains the linear element Y_p and the noise source n. The element $Y_p(j\omega)$, which is called the pilot describing function,[1] is a linear constant-coefficient system with a frequency response dependent on the input e(t).

[1]Technically, $Y_p(j\omega)$ represents a random input describing function because random, rather than sinusoidal, signals are used here (see ref. 3). Also, to avoid additional notation, terms such as $Y(j\omega)$ will be used to represent both the transfer functions of linear systems and the describing functions of nonlinear systems.

The term $n(t)$ represents the difference between output of the pilot, $c(t)$, and output of the describing function $Y_p(j\omega)$ driven by $e(t)$. Thus $n(t)$ accounts for remnant terms such as nonlinearities, time variations, and additive noise in the output of the pilot.

The controlled system is mathematically characterized by the constant linear element Y_c and the noise source i. The time history $i(t)$ accounts for nonlinearities and time variations in the controlled element, time-varying commands, and all disturbances from aerodynamics, propulsion, etc., external to the pilot.

Identification Error Using Standard Methods

Several methods (e.g., refs. 4-10) have been used to compute, from given records of $e(t)$ and $c(t)$, a describing function $\hat{Y}_m(j\omega)$ that represents the best linear relationship between $e(t)$ and $c(t)$. Best here means that the integral of the squared residual, $\int \varepsilon^2(t)dt$, is minimized over a given record length, where $\varepsilon(t)$ is the difference between the actual record $c(t)$ and the output of the system $\hat{Y}_m(j\omega)$ excited by $e(t)$. The measurements $\hat{Y}_m(j\omega)$ may differ somewhat between methods because each method uses slightly different approximations and model forms in computer processing. Generally, the measurements of $\hat{Y}_m(j\omega)$ will be near the following ideal describing function $Y_m(j\omega)$ that represents the best linear relationship between $e(t)$ and $c(t)$ for random stationary signals[2]:

$$\hat{Y}_m(j\omega) \approx Y_m(j\omega) = \frac{\Phi_{ec}(j\omega)}{\Phi_{ee}(\omega)} \tag{1}$$

In this equation, $\Phi_{ec}(j\omega)$ is the cross-power spectrum between $e(t)$ and $c(t)$ and $\Phi_{ee}(\omega)$ is the power density spectrum of $e(t)$. In identifying the pilot describing function with these types of methods, previous studies (e.g., refs. 4 and 9) have shown that there is a difference between the measured describing function $Y_m(j\omega)$ and the actual describing function $Y_p(j\omega)$. This difference, or "identification error," can be shown by delineating the components of the cross-power spectrum: $\Phi_{ec}(j\omega) = Y_p(j\omega)\Phi_{ee}(\omega) + \Phi_{en}(j\omega)$. Substituting these components into equation (1) yields

$$Y_m(j\omega) = Y_p(j\omega) + \underbrace{\frac{\Phi_{en}(j\omega)}{\Phi_{ee}(\omega)}}_{\text{error}} \tag{2}$$

Equation (2) shows that any cross-correlation $\Phi_{en}(j\omega)$ will contribute an error in identification. Such a correlation does exist during closed-loop control because $n(t)$ transfers through $Y_c(j\omega)$ and thus appears as a component of $e(t)$. If $n(t)$ is much smaller than $i(t)$, the ratio $\Phi_{en}(j\omega)/\Phi_{ee}(\omega)$ will be small and the measured transfer function $Y_m(j\omega)$ will be near the true

[2]If the measurement has the constraint to identify only physically realizable systems, then, as shall be pointed out later, $Y_m(j\omega)$ is written in a slightly different form.

value $Y_p(j\omega)$. However, if $n(t)$ is much larger than $i(t)$, the ratio $\Phi_{en}(j\omega)/\Phi_{ee}(\omega)$ will be significant and the measured describing function $Y_m(j\omega)$ will be very different from $Y_p(j\omega)$. For routine flight-test conditions, where $n(t)$ may be much larger than $i(t)$, it is necessary to find some means of reducing this error. Such a technique will be outlined next.

Use of a Time Shift in Identification

Previous studies (e.g., refs. 5-7) have considered the use of a time shift during the computer processing to account for the effective time delay of the pilot. This time shifting represents only a slight modification to the identification methods in figure 1.

This time-shifting technique illustrated in figure 2 involves the following steps in the computing process.

1. The input signal $e(t)$ is shifted with respect to $c(t)$ by an amount λ, where λ is equivalent to the time delay of the pilot.

2. The describing function $\hat{Y}_m(j\omega)$ is determined using the shifted data from step (1).

3. The estimated transfer function is determined from the measured transfer function as

$$\hat{Y}_p(j\omega) = e^{-\lambda j\omega}\hat{Y}_m(j\omega)$$

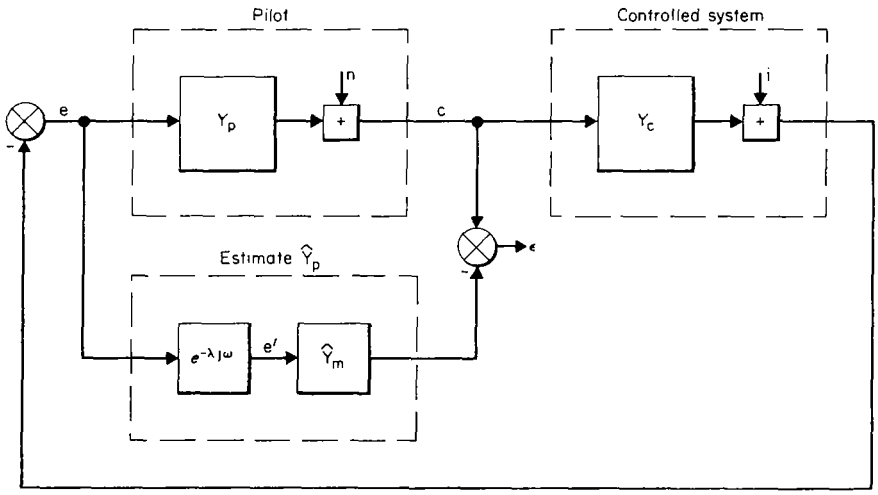

Figure 2.- The use of a time shift λ in identification.

Although previous studies have considered this time-shifting technique, it was apparently not observed that this technique would strongly influence the errors in identification. This report shows that when this technique is used with a measurement method in which $\hat{Y}_m(j\omega)$ is constrained to be

physically realizable,[3] then the identification error due to the correlation of e(t) with n(t) can be reduced. This reduction will be shown in the next section where the identification error to be expected with this computing process will be analyzed.

ANALYSIS OF IDENTIFICATION ERROR

The reduction of the identification error by the foregoing computer processing will be illustrated from two points of view. First, a general analysis will show why the time shift λ reduces the identification error. The second analysis will develop equations to show, in more detail, the amount the error is reduced. The following analysis is presented using the frequency domain. A similar analysis is presented in appendix A using the time domain.

General Analysis

To illustrate the reduction in identification error, equation (1) is rewritten as

$$\hat{Y}_m(j\omega) \approx Y_m(j\omega) = \frac{F[R_{ec}(\tau)]}{F[R_{ee}(\tau)]} = \frac{\int_{-\infty}^{\infty} R_{ec}(\tau)e^{-\tau j\omega}\, d\tau}{\int_{-\infty}^{\infty} R_{ee}(\tau)e^{-\tau j\omega}\, d\tau} \tag{3}$$

where $F[R_{ec}(\tau)]$ represents the Fourier transform of the cross-correlation function $R_{ec}(\tau)$ and $F[R_{ee}(\tau)]$ represents the Fourier transform of the autocorrelation function $R_{ee}(\tau)$. Representative curves[4] of the measured quantities $R_{ec}(\tau)$ and $R_{ee}(\tau)$ are sketched in figure 3(a). The error contribution $R_{en}(\tau)$, contained in $R_{ec}(\tau)$, is also shown for comparison.

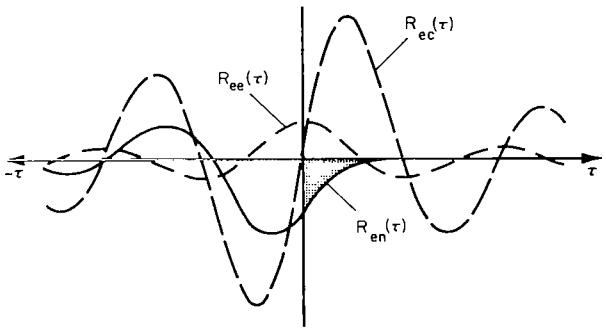

(a) No time shift; $\lambda = 0$

Figure 3.- Effect of time shift on correlation functions.

Now consider those measurement methods that have the constraint of physical realizability. These methods used only data for positive values of τ, and, accordingly, the measured transfer function is

[3]This constraint is inherent in the computer processing for most time-domain measurement methods such as cross-correlation (refs. 4, 8, and 9), orthogonal filters (refs. 4, 5, and 7), and parameter trackers (refs. 4, 6, and 10). Most frequency domain measuring methods using cross-spectral computing programs (ref. 1) usually do not contain this constraint. However, such a constraint could probably be incorporated.

[4]These data are from example 1, which will be discussed later.

$$Y_m(j\omega) = \frac{\int_0^\infty R_{ec}(\tau)e^{-\tau j\omega}\,d\tau}{\int_0^\infty R_{ee}(\tau)e^{-\tau j\omega}\,d\tau} \tag{4}$$

and if the individual terms (see eq. (2)) are substituted for $R_{ec}(\tau)$,

$$Y_m(j\omega) = Y_p(j\omega) + \underbrace{\frac{\int_0^\infty R_{en}(\tau)e^{-\tau j\omega}\,d\tau}{\int_0^\infty R_{ee}(\tau)e^{-\tau j\omega}\,d\tau}}_{\text{error}} \tag{5}$$

With this constraint, only that portion of $R_{en}(\tau)$ for positive values of τ (shown by the shaded region in fig. 3(a)) contributes an error in identification.

Let us next introduce the time shift λ as presented in figure 2. This time shift is applied so that the shifted input data are $e'(t) = e(t - \lambda)$. The effect of this time shift is illustrated in figure 3(b) where the functions $R_{e'n}(\tau)$, $R_{e'c}(\tau)$, and $R_{e'e'}(\tau)$ resulting from the shifted input data are presented. It is shown that the addition of this time shift causes the quantities $R_{e'c}(\tau)$, and $R_{e'n}(\tau)$ to be shifted by the amount λ with respect to $R_{e'e'}(\tau)$. Now it is apparent that the error contribution of $R_{e'n}(\tau)$, for the positive values of τ, is reduced and includes only the small shaded area in figure 3(b). The actual value for the error term is

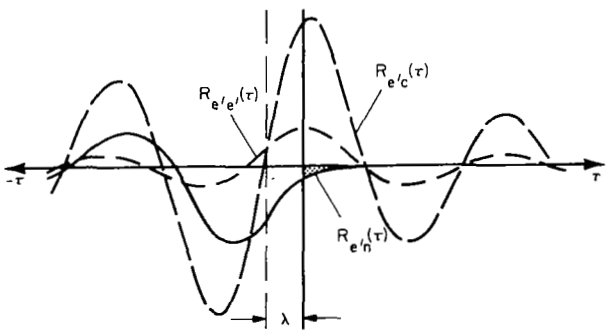

(b) With time shift λ

Figure 3.- Concluded.

$$\frac{\int_0^\infty R_{e'n}(\tau)e^{-\tau j\omega}\,d\tau}{\int_0^\infty R_{e'e'}(\tau)e^{-\tau j\omega}\,d\tau} = \frac{\int_0^\infty R_{en}(\tau + \lambda)e^{-\tau j\omega}\,d\tau}{\int_0^\infty R_{ee}(\tau)e^{-\tau j\omega}\,d\tau} \tag{6}$$

In general, $R_{en}(\tau)$ will decrease for positive values of τ. Therefore, note that the error contribution $\int_0^\infty R_{en}(\tau + \lambda)e^{-\tau j\omega}\,d\tau$ will be reduced as λ is increased. Further, the error contribution will be zero if $R_{en}(\tau)$ is zero for values of τ greater than λ.

This general discussion has attempted to give some physical insight into why the time shift λ reduces the error in identification. We will now turn our attention to a more detailed analysis to determine the amount the error can be reduced.

Detailed Analysis

In this section, we will derive formulas that show the reduction in identification error as a function of the primary variables within the control loop. As noted earlier, we will consider the use of a time shift λ in the identification and consider measurement methods in which $\hat{Y}_m(j\omega)$ is constrained to be physically realizable.

To mathematically represent a measured describing function $\hat{Y}_m(j\omega)$ that is constrained to be physically realizable, we can utilize the relationship used with the Wiener-Hopf equation (ref. 11). Using this relationship for physically realizable systems, equation (1) is written

$$\hat{Y}_m(j\omega) \approx Y_m(j\omega) = \frac{1}{\Phi^{+}_{ee}(j\omega)} \left[\frac{\Phi_{ec}(j\omega)}{\Phi^{-}_{ee}(j\omega)} \right]_{+} \tag{7}$$

where

$\Phi_{ee}(\omega) = \Phi^{+}_{ee}(j\omega)\Phi^{-}_{ee}(j\omega)$

$\Phi^{+}_{ee}(j\omega)$ has poles or zeros only in the left-half plane

$\Phi^{-}_{ee}(j\omega)$ has poles or zeros only in the right-half plane

$[\ ]_{+}$ has poles only in the left-half plane

This follows the usual form, which implies that the direct transform of a time function that is stable and zero for negative time will have all its poles in the left-half plane (LHP).

Now we introduce the time shift λ as illustrated in figure 2 and define the shifted data as $e'(t) = e(t - \lambda)$. Because $\Phi_{e'c}(j\omega) = e^{\lambda j\omega}\Phi_{ec}(j\omega)$ and $\Phi_{e'e'}(\omega) = \Phi_{ee}(\omega)$, we can write the measured transfer function as

$$Y_m(j\omega) = \frac{1}{\Phi^{+}_{ee}(j\omega)} \left[\frac{e^{\lambda j\omega}\Phi_{ec}(j\omega)}{\Phi^{-}_{ee}(j\omega)} \right]_{+} \tag{8}$$

As shown in figure 2, we can define the estimated describing function in terms of the measured describing function, $\hat{Y}_p(j\omega) = e^{-\lambda j\omega}\hat{Y}_m(j\omega)$. And if we assume that there is no modeling error, that is, $\hat{Y}_m(j\omega) = Y_m(j\omega)$, then a theoretical expression for the estimated describing function is

$$\hat{Y}_p(j\omega) = \frac{e^{-\lambda j\omega}}{\Phi^{+}_{ee}(j\omega)} \left[\frac{e^{\lambda j\omega}\Phi_{ec}(j\omega)}{\Phi^{-}_{ee}(j\omega)} \right]_{+} \tag{9}$$

Introducing the individual terms for $\Phi_{ec}(j\omega)$ (see eq. (2)), we have

$$\hat{Y}_p(j\omega) = \frac{e^{-\lambda j\omega}}{\Phi^+_{ee}(j\omega)}\left[e^{\lambda j\omega}Y_p(j\omega)\Phi^+_{ee}(j\omega)\right]_+ + \frac{e^{-\lambda j\omega}}{\Phi^+_{ee}(j\omega)}\left[\frac{e^{\lambda j\omega}\Phi_{en}(j\omega)}{\Phi^-_{ee}(j\omega)}\right]_+ \tag{10}$$

The impulse response function of Y_p is assumed to be zero for time less than a value of τ_p and, so long as λ is less than or equal to τ_p, the term $e^{\lambda j\omega}Y_p(j\omega)$ has poles only in the LHP. Simplifying equation (10) with this assumption, we obtain

$$\hat{Y}_p(j\omega) = Y_p(j\omega) + \frac{e^{-\lambda j\omega}}{\Phi^+_{ee}(j\omega)}\left[\frac{e^{\lambda j\omega}\Phi_{en}(j\omega)}{\Phi^-_{ee}(j\omega)}\right]_+ \tag{11}$$

The term $\Phi_{ee}(\omega)$ consists of contributions from two sources: $i(t)$ and $n(t)$. The maximum error can be determined by assuming $i(t) = 0$ (ref. 4). With this assumption and using basic closed-loop relationships (ref. 11), let us define

$$\Phi^+_{ee}(j\omega) = \frac{-Y_c(j\omega)\Phi^+_{nn}(j\omega)}{1 + Y_pY_c(j\omega)} \tag{12}$$

$$\Phi^-_{ee}(j\omega) = \frac{-Y_c(-j\omega)\Phi^-_{nn}(j\omega)}{1 + Y_pY_c(-j\omega)} \tag{13}$$

$$\Phi_{en}(j\omega) = \frac{-Y_c(-j\omega)\Phi^+_{nn}(j\omega)\Phi^-_{nn}(j\omega)}{1 + Y_pY_c(-j\omega)} \tag{14}$$

These definitions assume that $Y_c(j\omega)$ is minimum phase (i.e., contains no time delay or zeros in the RHP). The case in which $Y_c(j\omega)$ is a nonminimum phase will be illustrated at the end of this section.

Y_c Minimum phase.- From the foregoing assumptions, which cover a variety of piloted control situations, we find that

$$\hat{Y}_p(j\omega) = Y_p(j\omega) - \frac{\left[e^{\lambda j\omega}\Phi^+_{nn}(j\omega)\right]_+}{e^{\lambda j\omega}\Phi^+_{nn}(j\omega)}\left[\frac{1}{Y_c(j\omega)} + Y_p(j\omega)\right] \tag{15}$$

where now the error is conveniently expressed as a function of $\Phi_{nn}^{+}(j\omega)$, the excitation noise source. In equation (15), the terms $[e^{\lambda j\omega}\Phi_{nn}^{+}(j\omega)]_{+}$ and $\Phi_{nn}^{+}(j\omega)$ can be evaluated as shown in the following equation:

$$\hat{Y}_p(j\omega) = Y_p(j\omega) - \frac{\int_0^\infty R_{nn}(\tau + \lambda)e^{-\tau j\omega}\, d\tau}{\int_0^\infty R_{nn}(\tau)e^{-\tau j\omega}\, d\tau}\left[\frac{1}{Y_c(j\omega)} + Y_p(j\omega)\right]e^{-\lambda j\omega} \qquad (15a)$$

The contribution to the error term includes that portion of $R_{nn}(\tau)$ for values greater than λ (shaded area in fig. 4). It is seen that this contribution to the error term will be reduced as λ is increased. (However, this theoretical derivation holds only for those values of λ less than or equal to τ_p.)

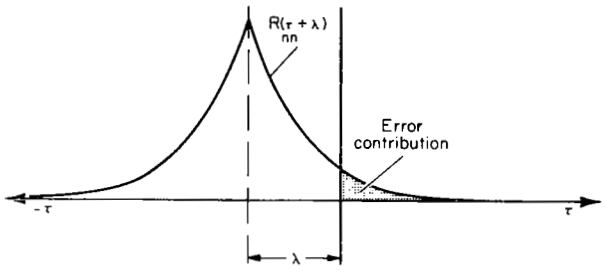

Figure 4.- Reduction of error contribution with λ.

Equation (15a) indicates those conditions under which the identification error will be small. For instance, note that if λ is positive and if $n(t)$ is white noise ($R_{nn}(\tau)$ is an impulse at $\tau = 0$), then $\int_0^\infty R_{nn}(\tau + \lambda)e^{-\tau j\omega}\, d\tau$ is zero and there will be no error in identification. More generally, the identification error will be zero if

$$R_{nn}(\tau) = 0 \quad \text{for} \quad \tau > \lambda \qquad (16)$$

where

$$\lambda \leq \tau_p$$

This result appears to have significance for many applications. The most important point is that when these conditions are met, a describing function $Y_p(j\omega)$ within a feedback system can theoretically be measured with the system excited only by the internal noise $n(t)$.

In most realistic situations, $R_{nn}(\tau)$ will not be identically zero for values of $\tau > \lambda$. We will next show, however, that the identification error can be reduced, and in some cases be made quite small, with more realistic forms of $R_{nn}(\tau)$. For example, assume that the noise $n(t)$ takes the form $R_{nn}(\tau) = Ke^{-\alpha|\tau|}$ which, for small α, would be narrow-band (nonwhite) noise. This form agrees quite well with some experimental measurements of the pilot remnant. (For instance, this exponential form with $\alpha = 5\ \text{sec}^{-1}$ agrees with the measured $n(t)$ in references 3 and 12.) With this form, we can evaluate the constant factor of equation (15) as

$$\frac{[e^{\lambda j\omega}\Phi_{nn}^{+}(j\omega)]_{+}}{\Phi_{nn}^{+}(j\omega)} = \frac{\int_0^\infty Ke^{-(\lambda+\tau)\alpha}e^{-j\omega\tau}\, d\tau}{\int_0^\infty Ke^{-\alpha\tau}e^{-j\omega\tau}\, d\tau} = e^{-\alpha\lambda}$$

and arrive at

$$\hat{Y}_p(j\omega) = Y_p(j\omega) - e^{-\alpha\lambda}\left[\frac{1}{Y_c(j\omega)} + Y_p(j\omega)\right]e^{-\lambda j\omega} \tag{17}$$

The error term on the right side of the equation is a function of the magnitude of the constant factor $e^{-\alpha\lambda}$. As λ increases and if α is large (near white noise), then $\hat{Y}_p(j\omega) \simeq Y_p(j\omega)$. Conversely, if $\lambda = 0$, then the result is identical to that shown in reference 4: $\hat{Y}_p(j\omega) = -1/Y_c(j\omega)$.

Y_c Nonminimum phase.- Let us define the nonminimum phase terms as $e^{-\tau_c j\omega}$ to represent any pure time delay in $Y_c(j\omega)$ and $N_c^-(j\omega)$ to represent any RHP zeros in $Y_c(j\omega)$. Then, by including these terms in equations (12) to (14), the estimated describing function becomes

$$\hat{Y}_p(j\omega) = Y_p(j\omega) - \frac{\left[e^{(\lambda+\tau_c)j\omega}\Phi_{nn}^+(j\omega)N_c^-(-j\omega)/N_c^-(j\omega)\right]_+}{e^{(\lambda+\tau_c)j\omega}\Phi_{nn}^+(j\omega)N_c^-(-j\omega)/N_c^-(j\omega)}\left[\frac{1}{Y_c(j\omega)} + Y_p(j\omega)\right] \tag{18}$$

Note that, in this case, if $R_{nn}(\tau) = 0$ for $\tau > \tau_c$, then $Y_p(j\omega)$ need not have a time delay (and no time delay, λ, is required in the analysis) in order that the identification error be zero.

In this more general case, the identification error in equation (18) will be zero if

$$R_{nn}(\tau) = 0 \quad \text{for} \quad \tau > \lambda + \tau_c \tag{19}$$

where

$$\lambda \leq \tau_p$$

The identification error can be made small if the autocorrelation function of the internal noise $R_{nn}(\tau)$ is negligible for values of τ greater than the sum of the time delays $\lambda + \tau_c$. We can also note that the term $N_c^-(-j\omega)/N_c^-(j\omega)$ is representative of a Padé approximation to a time delay. Thus, any RHP zeros in $Y_c(j\omega)$ will tend to act as an additional effective time delay and will further reduce the identification error.

This analysis of the identification error indicates that the internal noise $n(t)$ need not be a hindrance to identification, but rather it will aid in the identification of feedback control systems if the conditions of equation (19) are met. This analysis also may have application in many other fields such as biology, economics, and chemical processes. Although these other applications are not considered in this report, they do contain time delays and some of the measurements can be made only with the noise introduced within these systems to be identified.

APPLICATIONS AND DISCUSSION

The use of the computing technique outlined in this report will be illustrated through the identification of two examples using simulation data and one example using actual flight data. Each example will illustrate a different point. With example 1, the foregoing theoretical results will be compared with experimental results. With example 2, a method for selecting the time shift λ will be illustrated. With example 3, an application using actual flight records from Gemini X will be illustrated.

The simulated systems for the first two-examples are shown in figure 5. The dynamics for these examples were simulated on a digital computer. The output of a random noise program was appropriately filtered to obtain the desired spectrum of $n(t)$. The resulting dynamic records of $e(t)$ and $c(t)$ were processed using the method described in appendix A. The experimentally determined $\hat{Y}_p(j\omega)$ to be presented for these simulated examples represents the average values obtained from 12 separate 20-second runs.

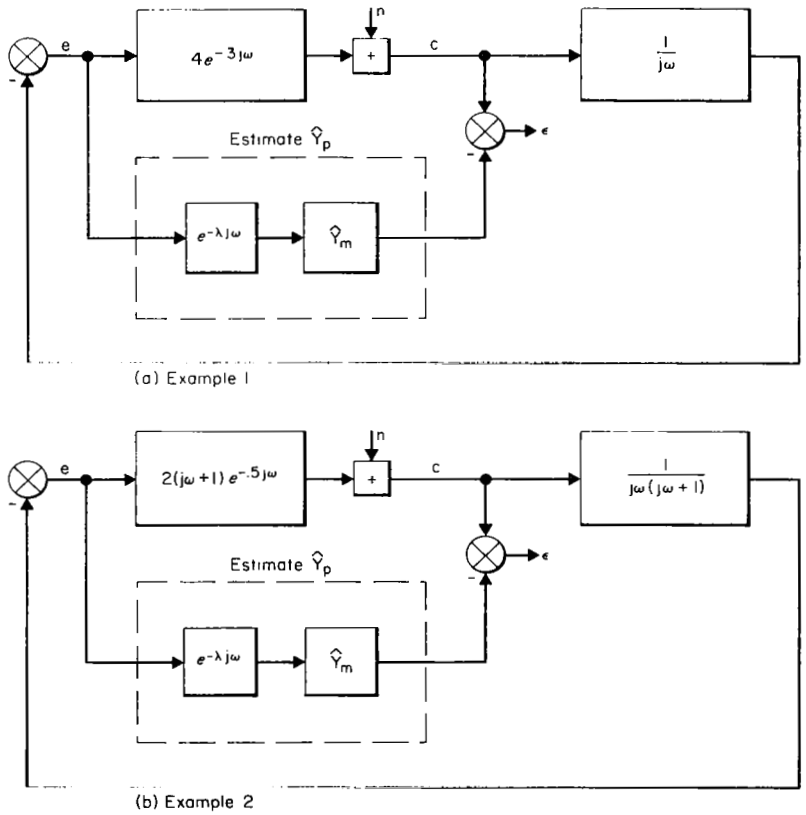

Figure 5.- System examples used to illustrate identification technique.

Example 1: Comparison of Theory With Experiment

To illustrate the theory, the system in figure 5(a) was simulated and an identification was made on the known model. The pilot model and controlled element were $Y_p(j\omega) = 4e^{-0.3j\omega}$ and $Y_c(j\omega) = 1/j\omega$. The measurements were made with no external disturbance, $i(t) = 0$, and with the only excitation being the internal noise source, $n(t)$. Two forms of the noise spectrum were considered: an $n(t)$ with a spectrum that approximates white noise to illustrate the condition from equation (16) for no identification error, and with a spectrum whose autocorrelation function is $R_{nn}(\tau) = e^{-\alpha|\tau|}$ to illustrate the theoretical results from equation (17) for an expected identification error.

Internal white noise.- For this case, the excitation source $n(t)$ had a spectrum near white noise. The time shift used in the computer processing was taken at $\lambda = 0.2$ sec. These conditions meet those specified for equation (16). According to equation (16), the estimation technique will identify the actual system, $\hat{Y}_p(j\omega) = 4e^{-0.3j\omega}$.

Figure 6(a) presents the experimentally determined magnitude $|\hat{Y}_p(j\omega)|$ and phase angle $\angle \hat{Y}_p(j\omega)$ as functions of frequency. Also shown for comparison are the magnitude $|Y_p(j\omega)|$ and phase angle $\angle Y_p(j\omega)$ of the actual system. The estimated amplitude $|\hat{Y}_p(j\omega)|$ varies ± 0.5 dB about the actual value for frequencies to about 9 rad/sec and the phase angle $\angle \hat{Y}_p(j\omega)$ is within $\pm 0.5°$ of the actual value. These differences appear to be within the experimental accuracies of the simulation. These results substantiate the theoretical conclusion that it is possible to identify the describing function of a system that is excited by noise $n(t)$ introduced within the system.

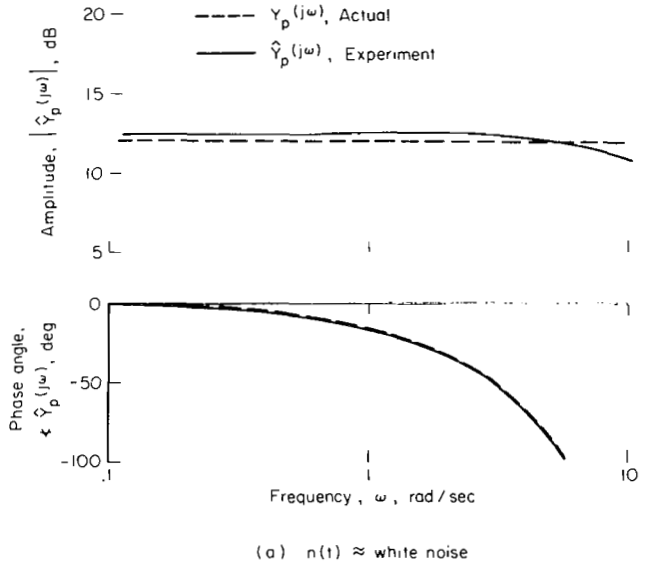

(a) $n(t) \approx$ white noise

Figure 6.- Identification of example 1; $\lambda = 0.2$ sec.

Internal nonwhite noise.- This case uses the same control elements and the same value $\lambda = 0.2$ sec as in the previous case. However, the assumed noise spectrum has a more realistic form $R_{nn}(\tau) = e^{-5|\tau|}$. For this case, the theory (eq. (17)) predicts the following estimated describing function:

$$\hat{Y}_p(j\omega) = \underbrace{4e^{-0.3j\omega}}_{Y_p(j\omega)} - \underbrace{0.37(j\omega + 4e^{-0.3j\omega})e^{-0.2j\omega}}_{\text{error}} \qquad (20)$$

This theoretical value of $\hat{Y}_p(j\omega)$ is presented in figure 6(b) along with the $\hat{Y}_p(j\omega)$ obtained from the experimental data. Also shown for comparison are the describing functions of the actual system $Y_p(j\omega)$ and the negative inverse of the controlled element $-1/Y_c(j\omega)$. The experimentally derived $\hat{Y}_p(j\omega)$ in this figure is close to that predicted by the theory. We can see from this figure that the estimated magnitude $|\hat{Y}_p(j\omega)|$ is about 4 dB below the actual value, $|Y_p(j\omega)|$, at the lower frequencies and tends to give the appearance of lead (slope = 20 dB/decade) at the higher frequencies. Overall, the estimated magnitude tends toward $|1/Y_c(j\omega)|$ as predicted by equation (17). The estimated phase angle, however, agrees quite well with the actual value.

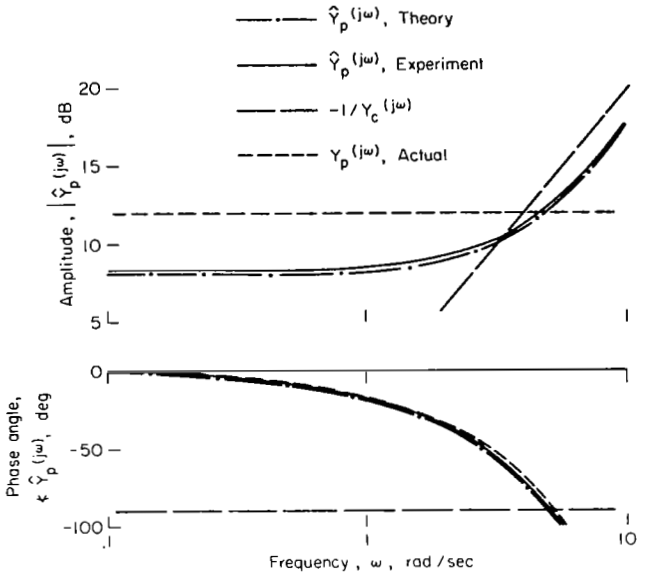

(b) $R_{nn}(\tau) = e^{-5|\tau|}$

Figure 6.- Concluded.

If a time shift were not used in this example, that is, if $\lambda = 0$, then the estimated describing function would be $\hat{Y}_p(j\omega) = -1/Y_c(j\omega)$, shown by the line in figure 6(b). It is interesting to note that with $\lambda = 0$, the value of the constant factor in the error term of equation (17) is $e^{-\alpha\lambda} = 1$. The value of this constant factor with $\lambda = 0.2$ sec, as shown in equation (20), is $e^{-\alpha\lambda} = 0.37$. Therefore, for $\lambda = 0.2$ sec the magnitude of the error term was reduced approximately 63 percent.

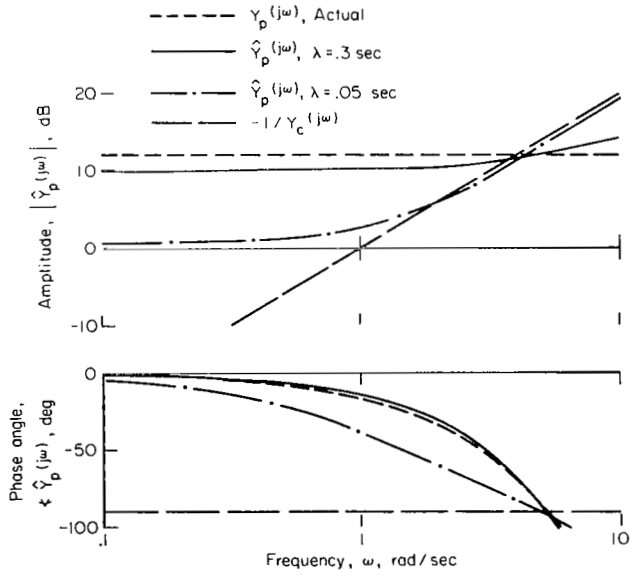

(a) Describing functions for $\lambda = .05$ sec and $\lambda = .3$ sec

Figure 7.- Effect of λ on identification; example 1; $R_{nn}(\tau) = e^{-5|\tau|}$.

Figure 7 illustrates the effect of λ on the identification error. The control system and spectrum of the excitation noise source, $R_{nn}(\tau) = e^{-5|\tau|}$, are the same as in the previous case. Experimental data, $\hat{Y}_p(j\omega)$, are shown in figure 7(a) for $\lambda = 0.05$ and 0.3 sec. Also shown for comparison are the actual system $Y_p(j\omega)$ and the negative inverse of the controlled element $-1/Y_c(j\omega)$. These experimental data illustrate the effect of λ predicted by the theory of equation (17). For small values of λ, in

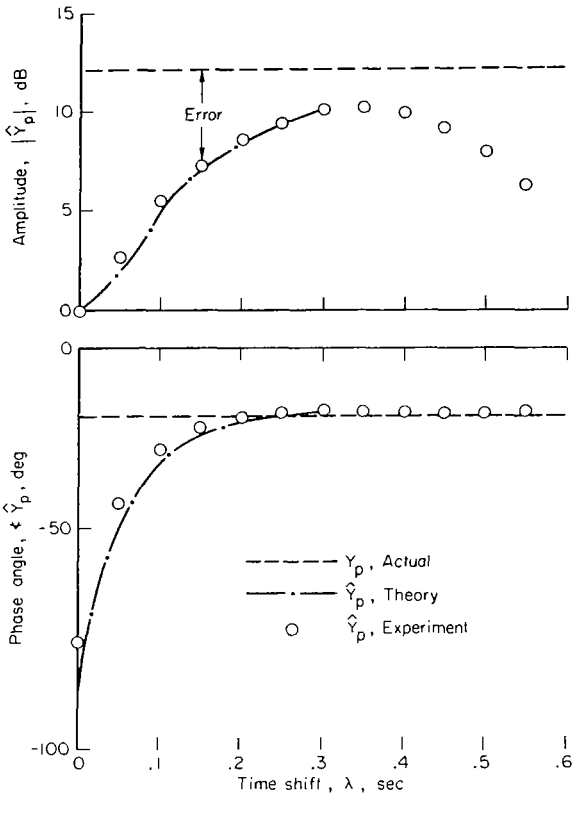

(b) Identification error for $\omega = 1$ rad/sec

Figure 7.- Concluded.

this case $\lambda = 0.05$ sec, the estimated describing function $\hat{Y}_p(j\omega)$ tends toward $-1/Y_c(j\omega)$. For larger values of λ, in this case $\lambda = 0.3$ sec, the estimated describing function is nearer the actual system describing function.

Experimental data are presented in figure 7(b) for several values of λ. These results are for one value of frequency, $\omega = 1$ rad/sec. In this figure, the experimental data are compared with the value for the actual system ($|Y_p| \approx 12$ dB and $\angle Y_p \approx -18°$). This comparison illustrates that the identification error decreases, as predicted by theory, to a value of $\lambda = 0.3$ sec, which is equal to τ_p. (The theory, as noted previously, is valid only for $\lambda \leq \tau_p$.) The error in $|\hat{Y}_p|$ is seen to increase for values of λ much larger than τ_p. This is to be expected because $\hat{Y}_p(j\omega)$ cannot properly model $Y_p(j\omega)$ with $\lambda > \tau_p$. These data indicate that the minimum error in $|\hat{Y}_p|$ occurs near a value of $\lambda \approx \tau_p$. The error in the phase angle $\angle Y_p$ is also seen to be very small at $\lambda \approx \tau_p$. As shown by this example, the value of λ should be near the time delay τ_p, to minimize the error identification.

We shall now recall an interesting point previously discussed (with eq. (2)) that can now be reinforced with experimental data. That is, the minimization of the identification error, as we have shown above, is not equivalent to finding the minimum value for the squared residual $\varepsilon^2(t)$ integrated over a a given run length. The following table presents the experimentally derived values of the fit term $\int\varepsilon^2(t)dt$, normalized with respect to $\int c^2(t)dt$, as a function λ. This table shows that the minimum value for the fit term is not at $\lambda = \tau_p = 0.3$ sec, but rather is at $\lambda = 0$. This is to be expected because with $\lambda = 0$ then $\hat{Y}_p(j\omega) = -1/Y_c(j\omega)$ and there is essentially perfect correlation between e(t) and c(t).

Time shift λ, sec	Normalized fit term $\int\varepsilon^2(t)dt/\int c^2(t)dt$
0	0.02
.1	.19
.2	.25
.3	.27
.4	.28
.5	.31

The fact that the minimum value for fit term $\int \varepsilon^2(t)dt$ appears at $\lambda = 0$ can lead to an erroneous interpretation in selecting the best value for λ. For instance, in previous studies (refs. 5-7), λ was selected by using that value which gave the best correlation between $e(t)$ and $c(t)$ (i.e., the minimum value for $\int \varepsilon^2(t)dt$). This previous method of selecting λ is unsatisfactory, however, because as we have just noted, if $n(t) >> i(t)$, then the best correlation is with $\lambda = 0$ and, in this case, $\hat{Y}_p(j\omega) = -1/Y_c(j\omega)$. An alternate method of selecting λ will be illustrated by the following example.

Example 2: A Method of Selecting the Time Shift

The previous example pointed out that the time shift λ should be near the time delay τ_p to minimize the identification error. The time delay τ_p may be approximately known in some situations (e.g., ref. 3) but, in general, its value will be unknown and will depend on the particular piloting task.

This example illustrates one method of selecting λ and will consider identification of the system shown in figure 5(b). The excitation noise source is the same as used in the previous case, $R_{nn}(\tau) = e^{-5|\tau|}$ and $i(t) = 0$; however, different forms for the pilot model $Y_p(j\omega) = 2(j\omega + 1)e^{-0.5j\omega}$ and controlled element $Y_c(j\omega) = \dfrac{1}{j\omega(j\omega + 1)}$ were chosen to demonstrate the identification of more complex dynamics. We will assume in this illustration that $Y_p(j\omega)$ is unknown. The objective will be to estimate the value of τ_p and then use this value for λ to obtain a best estimate for $\hat{Y}_p(j\omega)$.

For this example, the following procedure was used to estimate τ_p and thus, select λ.

1. Plot the estimated describing function for a selected value of λ.
2. Determine a transfer function that fits the plot, that is, $Y_p(j\omega) \approx (K_1 + K_2 j\omega)e^{-\tau_p j\omega}$, etc.
3. Note the value of estimated τ_p from step 2.
4. Repeat steps 1 through 3 until a value of λ approximately equal to the estimated τ_p is obtained.

The estimated describing functions for example 2 are presented in figure 8 for $\lambda = 0.2$ and 0.4 sec. Also shown for comparison is the describing function for $-1/Y_c(j\omega)$. These experimental data for $\lambda = 0.2$ and 0.4 sec follow the trends predicted by theory. The curve for the high value of λ (as compared to the curve for the lower values of λ) tends away from $-1/Y_c(j\omega)$. It was found for these data that any value of λ between $\lambda \approx 0.3$ sec and 0.8 sec resulted in approximately the same describing function as shown for $\lambda = 0.4$ sec. This estimated describing function can be approximated by a transfer function of the form $Y_p(j\omega) \approx (K_1 + K_2 j\omega)e^{-\tau_p j\omega}$. The

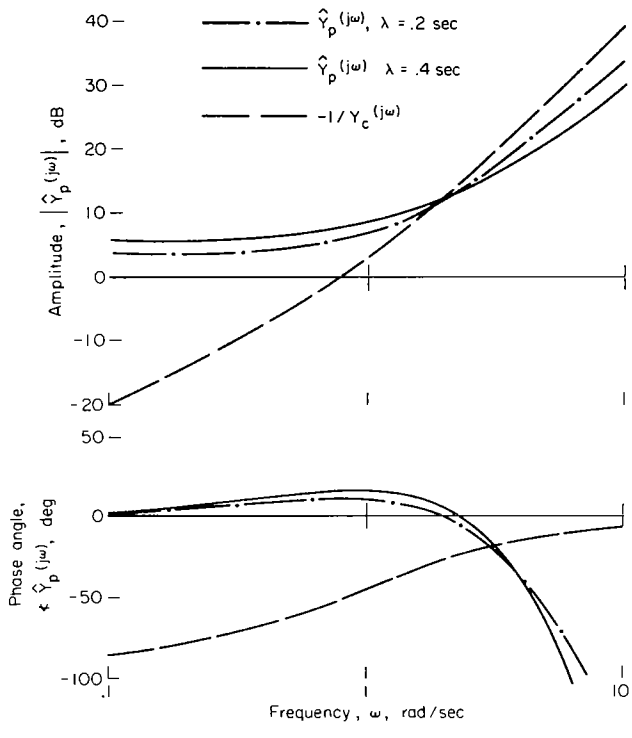

Figure 8.- Identification of example 2.

estimated τ_p values from fitting this transfer function to the plots (e.g., fig. 8) are presented in figure 9 for several values of λ. It is seen that λ is equal to the estimated time delay, τ_p, at $\lambda \approx 0.5$ sec. Therefore, λ = 0.5 sec should be selected for use in this example identification analysis. It is seen that for this example the method works well for estimating the actual τ_p.

Figure 10 compares the estimated describing function using λ = 0.5 sec with the actual describing function for example 2. Both the magnitude and the phase angle of the estimated describing function are seen to be near these values for the actual system. For this case, with λ = 0.5 sec, the theory of equation (17) predicts that the identification error in magnitude will be $e^{-\alpha\lambda}$ = 0.08. The experimental data shown in figure 10 appear to be within this 8-percent identification error as predicted by the theory.

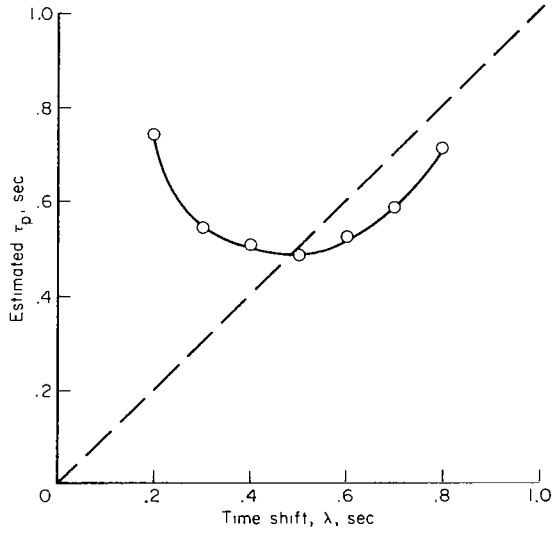

Figure 9.- Comparison of estimated τ_p with λ; example 2.

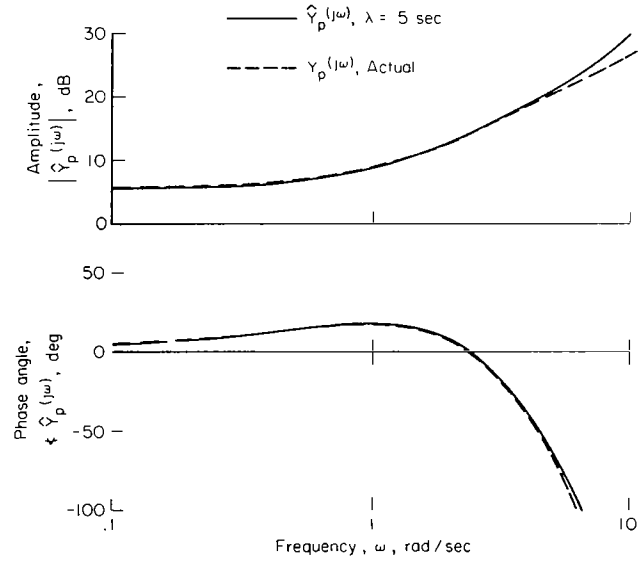

Figure 10.- Comparison of $\hat{Y}_p$ with Y_p; example 2.

Example 3: Flight Test Results From Gemini X

Flight data from Gemini X were analyzed to illustrate the application of this identification technique. In analyzing flight-test data, it is best to select a section of the record that contains disturbances external to the pilot. As noted earlier in the discussion following equation (2), external disturbances will tend to reduce the error in identification. The retrofire maneuver is a case in which external disturbances are introduced due to the unsymmetric ripple firing of the four retrorockets. The relationship of the pilot control task, the jet control system, and the disturbances during retrofire is illustrated schematically in figure 11.

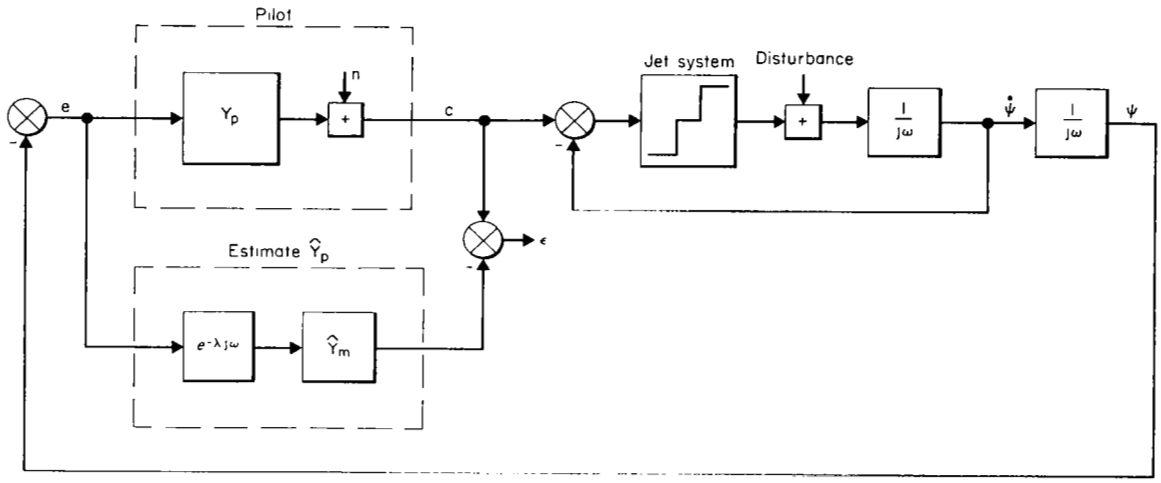

Figure 11.- Pilot describing function and flight control system; example 3.

During retrofire, the pilot controls the attitude about each of the three axes. There is no control coupling between these axes, and the pilot appears to treat them as three separate tasks. Of the three axes, the control about the yaw axis contained the best consistent correlation between attitude deviations, e(t), and control stick deflections, c(t). A time history of the recorded yaw control data is presented in figure 12. These control data will be used to illustrate the measurement of the pilot describing function during the retrofire of the Gemini spacecraft. (It should be emphasized that this was a normal retrofire maneuver and the astronaut had no prior knowledge of this identification attempt.)

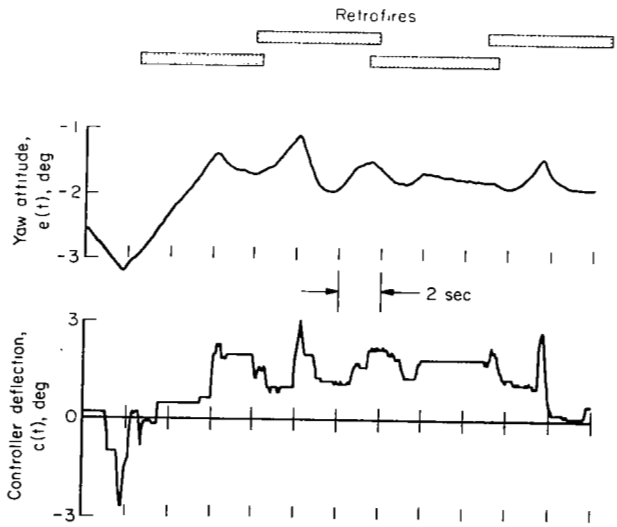

Figure 12.- Time history of yaw control task during retrofire.

The pilot describing function obtained for the data of figure 12 are

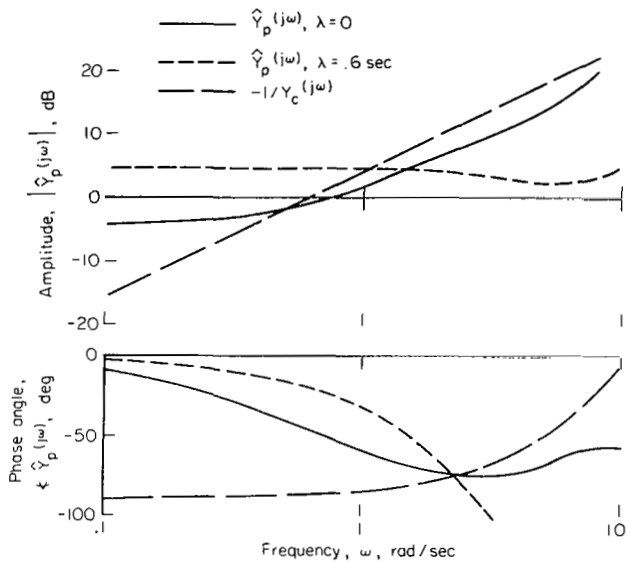

Figure 13.- Identification of pilot describing function; example 3.

presented in figure 13. Curves of magnitude, $|\hat{Y}_p(j\omega)|$, and phase angle, $\measuredangle \hat{Y}_p(j\omega)$, are presented as functions of frequency for $\lambda = 0$ and 0.6 sec. Also shown for comparison is the describing function[5] for $-1/Y_c(j\omega)$. The significance of this line was noted previously. The theory predicts that for $\lambda = 0$, the estimated describing function $\hat{Y}_p(j\omega)$ will tend toward $-1/Y_c(j\omega)$ as illustrated in figure 13. However, for this flight situation, $\hat{Y}_p(j\omega)$ does not coincide exactly with $-1/Y_c(j\omega)$ because of external disturbances due to the firing of the retrorockets and jet control system.

For $\lambda = 0.6$ sec, the estimated describing function $\hat{Y}_p(j\omega)$ tends away from the curve of $-1/Y_c(j\omega)$. Any value of λ from about $\lambda = 0.3$ to 0.7 sec resulted in approximately the same describing function as shown for $\lambda = 0.6$ sec. This estimated describing function can be approximated by a transfer function with a constant gain and a time delay, $Y_p(j\omega) \approx Ke^{-\tau_p j\omega}$.

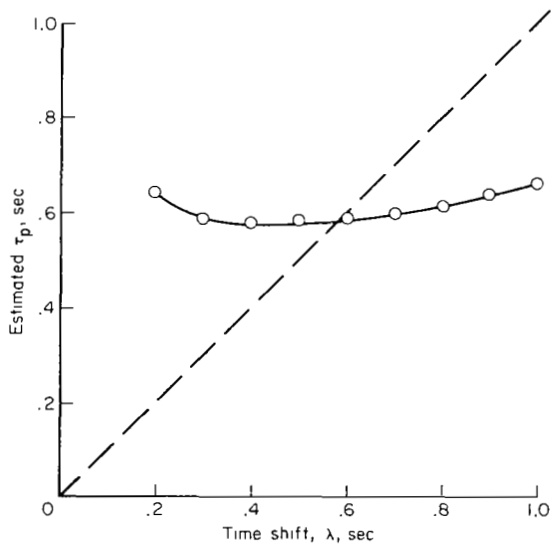

Figure 14.- Comparison of estimated τ_p with λ; example 3.

As noted previously, the value of λ that will minimize the identification error is dependent on the effective time delay of the pilot, τ_p. For these data, the procedure described previously was used to determine τ_p and, thus, select λ. With this procedure, τ_p was estimated by fitting the transfer function to the plots for several values of λ. These results are illustrated in figure 14 where the estimated τ_p values are presented as a function of λ. It is seen that λ is equal to the estimated time delay, τ_p, at $\lambda \approx 0.6$ sec. Therefore, $\lambda = 0.6$ sec was selected for use in this identification analysis.

One promising feature in analyzing the flight data is that the estimated describing functions are

[5]The describing function for the jet control system $Y_c(j\omega)$ was estimated from the flight data.

relatively insensitive to the exact value of the time shift, λ. For the estimated pilot describing functions (e.g., fig. 13), the plots are approximately the same for values of λ from about 0.3 to 0.7 sec (the estimated τ_p remained the same at about 0.6 sec). It appears that the exact value used for λ is not critical in this application of the identification technique.

The estimated describing function for $\lambda = 0.6$ sec (fig. 13) represents a constant gain system with an effective time delay. This result, although not directly comparable to the results from previous studies, appears reasonable. For instance, with a rate command system, which approximates the control system used in this situation, reference 1 has shown that the pilot describing function will be essentially a constant gain system with a time delay. The value τ_p for the three-axis flight data is higher than the value from the single-axis data in reference 1. However, other studies such as reference 13 have also shown higher values of τ_p when the pilot is involved in the complete task of monitoring the instrument panel and controlling about three separate axes.

Further analysis of this flight data is presented in appendix B. This appendix illustrates how the describing function of the pilot/control combination can be identified using the technique outlined in this report. This illustration is interesting because it presents the identification of an unknown system (i.e., pilot/control system) using only its own internal noise source for excitation.

CONCLUDING REMARKS

This report has shown that in measuring pilot describing functions the identification error due to the correlation of the input signal with the pilot output noise can be reduced by shifting the input data during the computer processing by an amount equivalent to the pilot time delay.

Both theory and experimental data have shown that the identification error can be made small if the autocorrelation function, $R_{nn}(\tau)$, of the internal noise source (pilot remnant) is negligible for τ greater than the sum of all effective time delays through the control loop (pilot plus controlled element). This finding has significance in general systems identification because, when these conditions are met, it is possible to measure the describing function of a system with feedback using only its own internal noise source for excitation.

Representative data selected from the retrofire portion of the Gemini X flight were analyzed using the technique outlined in this report. These results demonstrate the feasibility of identifying the pilot describing function from routine flight-test records.

Ames Research Center
National Aeronautics and Space Administration
Moffett Field, Calif., 94035, Jan. 15, 1969
125-19-01-42-00-21

APPENDIX A

TIME DOMAIN ANALYSIS AND COMPUTER PROCESSING

In this appendix, we will first use time domain analysis to outline the standard cross-correlation method (refs. 4 and 8). We shall then introduce the time shift λ and the computer processing equations used for the results in this report. The reduction in identification error due to λ will then be pointed out using these time domain equations. And, finally, we will discuss a modification of these computer processing equations to account for any data bias.

Standard Cross-Correlation Method

Let us consider analysis in the time domain in which the linear input-output relationship can be expressed in terms of a convolution integral

$$c(t) = \int_{o}^{t_m} h_p(\tau)e(t - \tau)d\tau + n(t) \tag{A1}$$

The $h_p(\tau)$ is the pilot impulse response function that is assumed to be zero for $\tau < 0$ (i.e., $h_p(\tau)$ is a real system) and also zero for $\tau > t_m$ (i.e., a finite memory time, t_m). A simple discrete approximation of equation (A1), to allow digital computation, is

$$c(k) = \Delta t \sum_{m=o}^{M} h_p(m)e(k - m) + n(k) \tag{A2}$$

where Δt is the discrete sampling time. The set of equations (A2) can be written in vector-matrix form as

$$\underline{c} = E\underline{h_p} + \underline{n} \tag{A3}$$

where

$$E = \Delta t \begin{bmatrix} e(k_o) & e(k_o - 1) & \cdots & e(k_o - M) \\ e(k_o + 1) & & & \\ \vdots & & & \vdots \\ \vdots & & & \vdots \\ \vdots & & & \vdots \\ e(K) & & \cdots & e(K - M) \end{bmatrix}$$

$$\underline{h}_p = \begin{bmatrix} h_p(0) \\ h_p(1) \\ h_p(2) \\ \vdots \\ h_p(M) \end{bmatrix} \qquad \underline{c} = \begin{bmatrix} c(k_o) \\ c(k_o + 1) \\ c(k_o + 2) \\ \vdots \\ c(K) \end{bmatrix} \qquad \underline{n} = \begin{bmatrix} n(k_o) \\ n(k_o + 1) \\ n(k_o + 2) \\ \vdots \\ n(K) \end{bmatrix}$$

An estimate of $\underline{h}_p$ can then be made, using standard least squares, by the formula

$$\hat{\underline{h}}_p = (E^T E)^{-1} E^T \underline{c} \tag{A4}$$

We should point out that the matrix to be inverted, $E^T E$, contains terms that represent discrete measurements of the autocorrelation function $R_{ee}(\tau)$, and that the vector $E^T \underline{c}$ contains terms that represent discrete measurements of the cross-correlation function $R_{ec}(\tau)$. For instance, the vector $E^T \underline{c}$ can be written in terms of the cross-correlation function as

$$E^T \underline{c} = \begin{bmatrix} \sum_{k=k_o}^{K} e(k)c(k) \\ \sum_{k=k_o}^{K} e(k-1)c(k) \\ \vdots \\ \sum_{k=k_o}^{K} e(k-M)c(k) \end{bmatrix} \approx \begin{bmatrix} R_{ec}(0) \\ R_{ec}(1) \\ \vdots \\ R_{ec}(M) \end{bmatrix} \tag{A5}$$

Use of a Time Shift in Computer Processing

The time shift λ is introduced into the computer processing by shifting the input data $e(k)$ a discrete number of time shifts L, where $\lambda = L\ \Delta t$. The linear pilot model is then expressed as

$$c(k) = \Delta t \sum_{m=o}^{M} h_p(L + m)e(k - m - L) + n(k) \tag{A6}$$

This form assumes that the impulse response h_p is zero for time less than λ. This form also assumes a memory time of $t_m = \lambda + M\ \Delta t$. For the results in this report, $M = 9$ and $\Delta t = 0.05$ sec. (Larger values of M were also tried with no significant changes in the results.)

Using the least-squares formulation, the impulse response function of the pilot was determined by the following matrix inversion on a digital computer:

$$\begin{bmatrix} \hat{h}_p(L) \\ \hat{h}_p(L+1) \\ \vdots \\ \hat{h}_p(L+M) \end{bmatrix} = (\Delta t)^{-1} \begin{bmatrix} \sum_{k=k_o}^{K} e^2(k-L) & \sum_{k=k_o}^{K} e(k-L)e(k-1-L) & \cdots & \sum_{k=k_o}^{K} e(k-L)e(k-M-L) \\ \sum_{k=k_o}^{K} e(k-1-L)e(k-L) & \sum_{k=k_o}^{K} e^2(k-1-L) & \cdots & \sum_{k=k_o}^{K} e(k-1-L)e(k-M-L) \\ \vdots & \vdots & \vdots & \vdots \\ \sum_{k=k_o}^{K} e(k-M-L)e(k-L) & \sum_{k=k_o}^{K} e(k-M-L)e(k-1-L) & \cdots & \sum_{k=k_o}^{K} e^2(k-M-L) \end{bmatrix}^{-1} \begin{bmatrix} \sum_{k=k_o}^{K} e(k-L)c(k) \\ \sum_{k=k_o}^{K} e(k-1-L)c(k) \\ \vdots \\ \sum_{k=k_o}^{K} e(k-M-L)c(k) \end{bmatrix} \tag{A7}$$

This time domain solution was further transformed into the frequency domain using the following approximation for the Fourier transform:

$$\hat{Y}_p(j\omega) = \underbrace{e^{-L\ \Delta t j\omega}}_{e^{-\lambda j\omega}} \underbrace{\Delta t \sum_{m=o}^{M} \hat{h}_p(L + m)e^{-m\ \Delta t j\omega}}_{\hat{Y}_m(j\omega)} \tag{A8}$$

Reduction in Identification Error With Time Shift

In order to show, using time domain analysis, that the time shift λ reduces the identification error, we can write equation (A4) as

$$\underline{\hat{h}}_p = \underline{h}_p + \underbrace{[E^T E]^{-1} E^T \underline{n}}_{\text{error}} \tag{A9}$$

The identification error, shown above in vector form, is due to the correlation of $e(k)$ with $n(k)$. The terms in the vector $E^T\underline{n}$ can be regarded as discrete values of the cross-correlation function $R_{en}(\tau)$.

$$E^T\underline{n} = \begin{bmatrix} \sum_{k=k_o}^{K} e(k)n(k) \\ \sum_{k=k_o}^{K} e(k-1)n(k) \\ \vdots \\ \sum_{k=k_o}^{K} e(k-M)n(k) \end{bmatrix} \approx \begin{bmatrix} R_{en}(0) \\ R_{en}(1) \\ \vdots \\ R_{en}(M) \end{bmatrix} \tag{A10}$$

If $R_{en}(\tau)$ is nonzero for $\tau \geq 0$, then the terms $R_{en}(m)$, $m \geq 0$, will be nonzero and there will be an identification error.

Now, introducing a discrete number of time shifts L, such as used in equation (A7), the vector $E^T\underline{n}$ becomes

$$E^T\underline{n} = \begin{bmatrix} \sum_{k=k_o}^{K} e(k-L)n(k) \\ \sum_{k=k_o}^{K} e(k-1-L)n(k) \\ \vdots \\ \sum_{k=k_o}^{K} e(k-M-L)n(k) \end{bmatrix} \approx \begin{bmatrix} R_{en}(L) \\ R_{en}(L+1) \\ \vdots \\ R_{en}(L+M) \end{bmatrix} \tag{A11}$$

We can see that this use of the time shift removes the terms $R_{en}(m)$, $0 \leq m < L$, and adds the terms $R_{en}(m)$, $M < m \leq M + L$. The terms that are

added generally are smaller than the terms removed; thus, the use of a time shift L, or the equivalent λ, reduces the identification error. (Time shifting will not significantly alter the matrix E^TE.) Further note that the identification error will be zero if $R_{en}(m)$ is zero for values of $m \geq L$.

Computer Processing With Data Bias

The data $c(k)$ and $e(k)$ obtained from routine flight tests will usually contain some type of long-term variation about which the short-period dynamics are to be estimated. (See, for instance, the flight-test data in fig. 12.) There may be a bias or drift in $e(k)$ because of instrumentation errors or because the pilot may be controlling about some nonzero value. There may be bias in $c(k)$ because of instrumentation errors or because the pilot must hold some nonzero offset with the controller (e.g., if the vehicle is out of trim). In the analysis of the flight-test records for this report, a bias term and a drift term were added to the foregoing formulation so that

$$c(k) = b_o + b_1 k\,\Delta t + \Delta t \sum_{m=o}^{M} h_p(L + m)e(k - L - m) + n(k)$$

The estimated constant bias term $\hat{b}_o$ and estimated drift term $\hat{b}_1$, along with the estimated impulse response function $\hat{h}_p(m)$, were determined by the least-squares solution. This new formulation required the inversion of an $M + 3$ square matrix instead of the $M + 1$ square matrix shown previously in equation (A7).

APPENDIX B

IDENTIFICATION OF THE PILOT/CONTROL DESCRIBING FUNCTION

The describing function of the pilot/control combination has been used extensively (e.g., ref. 1) to analyze the closed-loop dynamics of piloted systems. This appendix illustrates the use of the technique outlined in this report to identify the pilot/control describing function. This illustration will use the Gemini data presented previously in figure 12.

The describing function $\hat{Y}_x(j\omega)$ to be identified is shown in relationship to the pilot and the control system in figure 15. This describing function

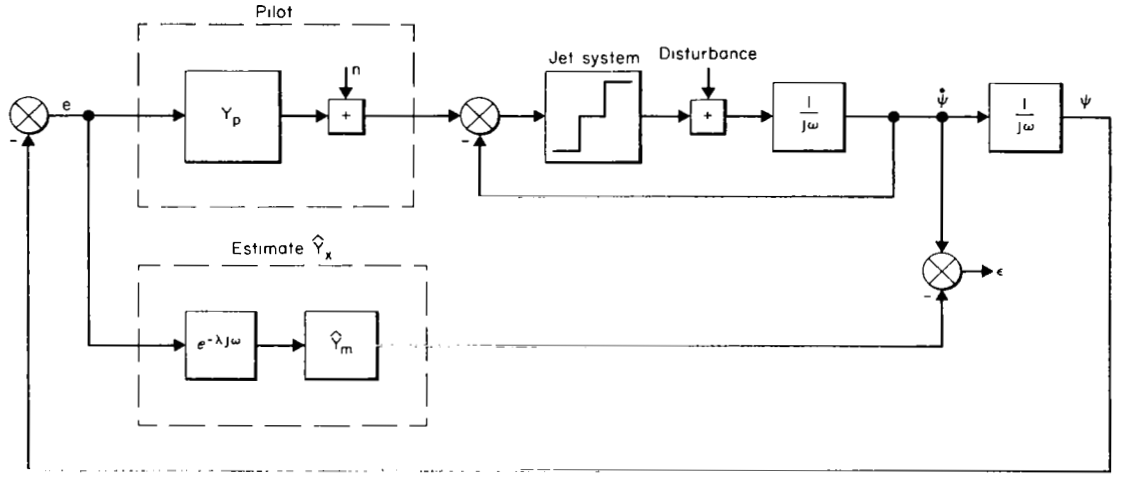

Figure 15.- The technique for identifying the pilot/control describing function.

was measured[1] between the attitude error signal $e(t)$ and the attitude rate signal $\dot{\psi}(t)$. The Bode plots obtained from these data are presented in figure 16. Curves of the estimated describing function $\hat{Y}_x(j\omega)$ are shown for $\lambda = 0$ and 0.7 sec. Also shown for comparison is the Bode plot for the negative inverse of the feedback path, $-j\omega$. The theory predicts that, for $\lambda = 0$, the estimated describing function will identify $-j\omega$ because, in this case, there are no disturbances external to the measured describing function. As

[1]It is interesting to observe that the identification of the pilot/control describing function required only a single channel of recorded data. The output signal used in the computer processing was the recorded yaw rate, $\dot{\psi}(t)$. The input signal was also determined from this same recorded data as

$$e(t) = -\int_0^t \dot{\psi}(\tau)d\tau + \text{bias} + \text{drift}$$

where the unknown bias and drift are accounted for by the method shown in appendix A.

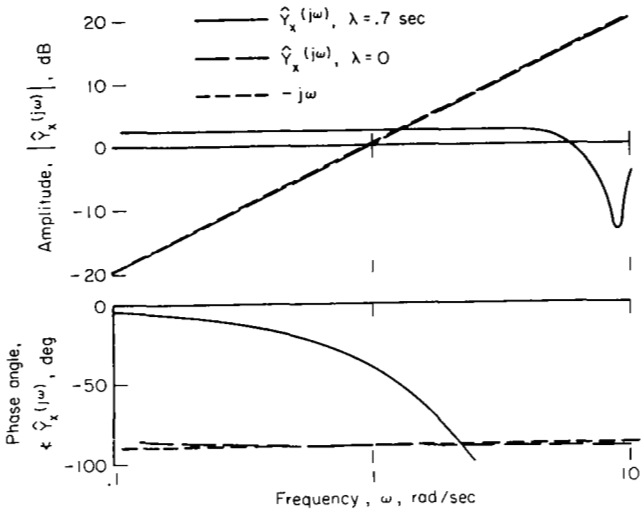

Figure 16.- Identification of pilot/control describing function.

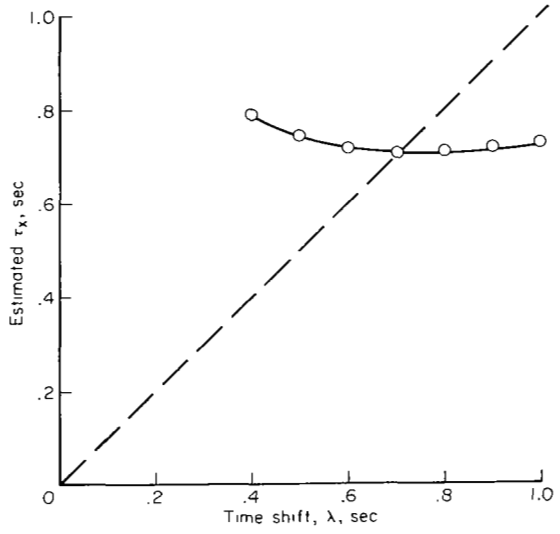

Figure 17.- Comparison of estimated τ_x with λ.

shown in figure 16, the curve for $\lambda = 0$ essentially coincides with the curve for $-j\omega$.

For increasing values of λ, the estimated describing function tends away from the curve of $-j\omega$. Any value of λ between 0.4 and 1.0 sec resulted in approximately the same Bode plot as shown for $\lambda = 0.7$ sec. The estimated describing function can be approximated by a describing function with a constant gain K_x and a time delay τ_x; $\hat{Y}_x(j\omega) \approx K_x e^{-\tau_x j\omega}$. The estimated values for τ_x are presented in figure 17 for several values of λ. We can see that λ is equal to the estimated τ_x at $\lambda \approx 0.7$ sec, so $\lambda = 0.7$ sec was selected for this analysis.

From the estimate $\hat{Y}_x(j\omega)$, we can determine the describing function for pilot/controlled element combination, $\hat{Y}_p\hat{Y}_c(j\omega)$. The describing function $\hat{Y}_x$ can be combined with the integration, $1/j\omega$, as shown in figure 15, to obtain

$$\hat{Y}_p\hat{Y}_c(j\omega) = \frac{\hat{Y}_x(j\omega)}{j\omega}$$

For the results from figure 16, the estimated describing function is $\hat{Y}_x(j\omega) \approx 1.3e^{-0.7j\omega}$ so that

$$\hat{Y}_p\hat{Y}_c(j\omega) \approx \frac{1.3e^{-0.7j\omega}}{j\omega}$$

This result appears reasonable. From previous studies such as reference 1, it has been shown that for a variety of controlled elements the pilot will control so that $Y_pY_c(j\omega) \approx \frac{K_x e^{-\tau_x j\omega}}{j\omega}$. This form is the same as found in the actual flight results. The actual value for the gain (a crossover frequency, K_x, of 1.3 rad/sec) is lower than predicted in reference 1 and the value for the effective time delay ($\tau_x \approx 0.7$ sec)

is higher than predicted in reference 1. Again, it is reasonable to expect (see refs. 10 and 13) that these differences can be attributed to the fact that in reference 1, the pilot was controlling only a simple single-axis task, whereas, for the actual flight data, the pilot was controlling about three axes and monitoring the complete instrument panel.

REFERENCES

1. McRuer, Duane; Graham, Dunstan; Krendel, Ezra; and Reisener, William, Jr.: Human Pilot Dynamics in Compensatory Systems. Tech. Rept. AFFDL TR-65-15, USAF, July 1965.

2. Newell, Fred D.; and Pietrzak, Paul E.: In-Flight Measurement of Human Response Characteristics. J. Aircraft, vol. 5, no. 3, May-June 1968, pp. 277-284.

3. McRuer, Duane T.; and Jex, Henry R.: A Review of Quasi-Linear Pilot Models. IEEE Transactions on Human Factors in Electronics, vol. HFE-8, no. 3, Sept. 1967, pp. 231-249.

4. Elkind, Jerome I.: Further Studies of Multiple Regression Analysis of Human Pilot Dynamic Responses; A Comparison of Analysis Techniques and Evaluation of Time-Varying Measurements. ASD-TDR-63-618, March 1964.

5. Elkind, Jerome I.; Starr, Edward A.; Green, David M.; and Darley, D. Lucille: Evaluation of a Technique for Determining Time-Invariant and Time-Variant Dynamic Characteristics of Human Pilots. NASA TN D-1897, 1963.

6. Todosiev, E. P.; Rose, R. E.; Bekey, G. A.; and Williams, H. L.: Human Tracking Performance in Uncoupled and Coupled Two-Axis Systems. NASA CR-532, 1966.

7. Wierwille, Walter W.; and Gagne, Gilbert A.: A Theory for the Optimal Deterministic Characterization of the Time-Varying Dynamics of the Human Operator. NASA CR-170, 1965.

8. Taylor, Lawrence W., Jr.: A Comparison of Human Response Modeling in the Time and Frequency Domains. Proceedings of the 3rd Annual NASA-University Conference on Manual Control. NASA SP-144, 1967, pp. 137-153.

9. Goodman, T. P.; and Reswick, J. B.: Determination of System Characteristics from Normal Operating Records. Transactions of the ASME, vol. 78, pp. 259-268, Feb. 1956.

10. Adams, James J.; Bergeron, Hugh P.; and Hurt, George J., Jr.: Human Transfer Functions in Multi-Axis and Multi-Loop Control Systems. NASA TN D-3305, 1966.

11. Newton, George C.; Gould, Leonard A.; and Kaiser, James F.: Analytical Design of Linear Feedback Controls. John Wiley and Sons, N. Y., 1957.

12. McDonnell, J. D.; and Jex, H. R.: A "Critical" Tracking Task for Man-Machine Research Related to the Operators Effective Time Delay. NASA CR-674, 1967.

13. Clement, W. F.; Jex, H. R.; and Graham, D.: Application of a System Analysis Theory for Manual Control Displays to Aircraft Instrument Landing. Paper presented at 4th Annual NASA-University Conference on Manual Control, Univ. of Mich., March 1968.

NASA-Langley, 1969 — 5 A-2993